Opto-Thermal Mathematical Modelling and Inverse Depth Profiling Using Genetic Algorithm

Yingxin Cui, Peng Xiao, Robert E. Imhof

School of Engineering, South Bank University, 103, Borough Road, London, SE13 0AA, UK

Abstract

The OTTER non-invasive measurement of water concentration depth profiles in human skin is important for development an understanding of its barrier function. In this paper, we present a new inverse method for analysing opto-thermal data to yield optical depth profiles, which is based on a new multi-layer mathematical model designed for opto-thermal skin data analysis. This has been combined with a novel inverse analysis technique using a Genetic Algorithm. The performance of the new approach is tested on both simulated data and in-vivo experimental skin data. We present the theoretical background and compare the analysis of typical measurements using the new approach with conventional analyses.

1. Introduction

Optothermal transient emission radiometry (OTTER) is a non-destructive, remote sensing measurement technology, which has been proven potentially attractive for biomedical studies[1]. Our previous work has shown that the data from OTTER measurements is information rich, and one meaningful characteristic we especially concern about is the sample's optical depth profile, which often reflects sample's inhomogeneity and can be correlated to concentration profiles of water or externally applied substances, depending on measurement protocol, excitation and detection wavelengths. However, due to the severely ill pose of the inverse calculation[2], the analysis of OTTER data is limited and scanty.

In this work, we investigate a new multilayered mathematical model and an inverse algorithm based on Genetic Algorithm, to extract the depth profile of optical absorption coefficient. A good agreement of the simulated and measured data indicates the acceptability of the model and the algorithm.

2. Multilayered Mathematical Modelling

In OTTER measurement, a pulsed laser is used as the excitation source to heat up the sample, and a fast infrared detector as a sensor to pick up the consequent changes of the thermal radiation due to this temperature increase in the sample near surface. A schematic diagram of an OTTER measurement is shown in Fig.1. The transient temperature field $\theta(z,t)$ can be expressed as[3]

$$\theta(z,t) = \int_0^\infty \theta(z,0) G(z,z';t,0)\, dz' \tag{1}$$

where $\theta(z,0)$ is the initial temperature field, and $G(z,z';t,0)$ is the Green function. The opto-thermal signal comes from the transient thermal emission, which can be calculated from

$$S(t) = \frac{\zeta E_0}{\rho C} \int_0^\infty \beta e^{-\beta z} \theta(z,t) dz \tag{2}$$

where β is the absorption coefficient for the emitted thermal radiation, C the specific heat, ρ the density, E_0 the energy density absorbed from the excitation pulse, and the parameter $\zeta = \zeta(\lambda_{em})$ includes factors that depend on the black body emission curve, detector sensitivity, focusing and alignment, but is independent of the properties of the sample per se.

In the simplest case of a homogeneous, semi-infinite sample, the initial temperature field and the signal can be expressed respectively as

$$\theta(z,0) = \frac{E_0 \alpha}{\rho C} e^{-\alpha z} \tag{3}$$

and

$$S(t) = \frac{\xi E_0 \alpha}{\rho C} e^{\alpha^2 Dt} erfc \sqrt{\alpha^2 Dt} \tag{4}$$

where α is the absorption coefficient for the excitation radiation, and D is the thermal diffusivity.

Whereas a lot of practical samples are not ideal enough to be treated as homogeneous, the new model discussed here is for samples with homogeneous thermal properties but with inhomogeneous optical properties. The sample is divided into N layers, which are perfectly connected with each other. Assume the absorption coefficient for excitation radiation of the sample is constant, but each layer of the sample has an absorption coefficient β_i for the emitted radiation, and a thickness of L_i. Then the signal turns to

$$
\begin{aligned}
S(t) &= \frac{\zeta E_0}{\rho C}\sum_{i=1}^{N}\int_{L_{i-1}}^{L_i}\beta_i e^{-\beta_i z}\theta(z,t)dz \\
&= \frac{E_0\alpha}{2\rho C}e^{t/\tau_\alpha}\left\{\sum_{i=1}^{N}\frac{e^{-(\alpha+\beta_i)L_{i-1}}}{\alpha+\beta_i}erfc\left(\frac{t/\tau_\alpha-\alpha L_{i-1}/2}{\sqrt{t/\tau_\alpha}}\right)-\frac{e^{-(\alpha+\beta_i)L_i}}{\alpha+\beta_i}erfc\left(\frac{t/\tau_\alpha-\alpha L_i/2}{\sqrt{t/\tau_\alpha}}\right)\right. \\
&\quad +\frac{e^{\left(\beta_i^2-\alpha^2\right)t/\alpha^2\tau_\alpha}}{\alpha+\beta_i}\left[erf\left(\frac{-2\beta_i t-\alpha^2 L_{i-1}\tau_\alpha}{2\alpha\sqrt{\tau_\alpha t}}\right)-erf\left(\frac{-2\beta_i t-\alpha^2 L_i\tau_\alpha}{2\alpha\sqrt{\tau_\alpha t}}\right)\right] \\
&\quad +\frac{e^{(\alpha-\beta_i)L_1}}{\alpha-\beta_i}erfc\left(\frac{t/\tau_\alpha+\alpha L_i/2}{\sqrt{t/\tau_\alpha}}\right)-\frac{e^{(\alpha-\beta_i)L_{i-1}}}{\alpha-\beta_i}erfc\left(\frac{t/\tau_\alpha+\alpha L_{i-1}/2}{\sqrt{t/\tau_\alpha}}\right) \\
&\quad \left.+\frac{e^{\left(\beta_i^2-\alpha^2\right)t/\alpha^2\tau_\alpha}}{\alpha-\beta_i}\left[erf\left(\frac{2\beta_i t+\alpha^2 L_i\tau_\alpha}{2\alpha\sqrt{\tau_\alpha t}}\right)-erf\left(\frac{2\beta_i t+\alpha^2 L_{i-1}\tau_\alpha}{2\alpha\sqrt{\tau_\alpha t}}\right)\right]\right\}
\end{aligned}
\tag{5}
$$

where $\tau_\alpha = {}^{1}\!/\!_{\alpha^2 D}$.

In the following algorithm, all the calculations are based on the based on the above model, normalized to its initial value $\left(S(t)/S(0)\right)$.

3. Inverse Algorithm

With N dimension vector $\vec{S}_m$ and $\vec{S}_c(\vec{\beta})$ ($\vec{\beta}=[\beta_1,\beta_2,\ldots,\beta_N]$) to denote the measurement signal data and calculated data, the OTTER inverse problem can be described as an optimisation problem Eq. (6), and in terms of property continuity of practical biomedical sample, it is a constraint optimisation problem.

$$
\begin{aligned}
&\textit{Minimize} \quad \left\|\vec{S}_m-\vec{S}_c(\vec{\beta})\right\|^2 \\
&\textit{Subject to} \quad \left|\beta_i-\beta_{i+1}\right|<C_\beta \qquad i=1,2,\ldots,N
\end{aligned}
\tag{6}
$$

where, $\|\cdot\|$ denotes the Euclidean distance, and C_β is the constant to keep the property continuity of sample.

Compare with other inverse algorithms[4], Genetic Algorithm (GA) can search complex and large state-spaces more efficiently, locate near optimal solutions more rapidly and allow additional constraints to be easily specified[5]. Due to the flexibility and versatility of GA in solving optimisation problems, GA is applied in this work. GAs are relatively new combinatorial search techniques based on mechanics of natural selection and natural genetics, which combines artificial survival of the fittest concept with genetic operations abstracted from nature. The basic structure of a GA is shown in Fig.2. First, an initial population of chromosomes for the GA is generated, usually in a random way. Then, the value of a function called fitness function is evaluated for each chromosome

of the population. After this, the genetic operators reproduction, crossover and mutation are used in succession, to create a new population of chromosomes for the next generation. The process of evaluation and creation of new successive generation is repeated until the satisfaction of a convenient termination condition.

Conventionally, most applications of GA to constraint optimisation problems have used the penalty function approach of handling constraints[6]. However, the penalty function approach involves a number of penalty parameters that must be set right in any problem to obtain feasible solutions. Different from the conventional methods, K. Deb[7] developed an efficient constraint handling method for GA based on the penalty function approach which does not require any penalty parameter. According to his fitness function, infeasible solutions are compared based on only their constraint violation. Here a binary GA is designed using K. Deb's method but with a few modifications. The fitness function is devised as following:

$$F(\vec{\beta}) = \begin{cases} \left\| \vec{S}_m - \vec{S}_c(\vec{\beta}) \right\|^2 & \text{if} \quad |\beta_i - \beta_{i+1}| < C_\beta \quad \forall i = 1,2,\ldots,N-1 \\ N + \sum_{i=1}^{N-1} \left\langle C_\beta - |\beta_i - \beta_{i+1}| \right\rangle & \text{otherwise} \end{cases} \tag{7}$$

where $\langle\ \rangle$ denotes the absolute value of the operand, if the operand is negative and returns a value zero, otherwise. And other GA parameters are defined as: population size = $10N$, maximum no. of generations = 100, generation gap = 0.9, and crossover probability = 0.7.

4. Results and Discussions

A. Simulation results

With constant thermal diffusivity and the absorption coefficient for the excitation radiation, one group of simulated data, calculated (with 5% white noise added) from one constant absorption coefficient (1.9×10^5) profile for the emitted thermal radiation of a ten layered model using Eq.(5), were used to test the new inverse algorithm. The sample is assumed to be divided equally with 1 μm length of each layer. The results in Fig.3 show obviously that the calculated data fit simulation signal data perfectly, and the calculated optical depth profile of β is relatively constant, which indicates the new algorithm is efficient for the constraint handling.

B. Measurement results

The measurements were performed at different skin sites on a conventional OTTER apparatus with a Q-switched ER:YAG laser (2.94 μm) and 13.1μm detection wavelength, and β gives information about hydration. The results are shown as Fig.4. In general, the skin of the forearm has more water and a higher hydration gradient than other sites, while nail has the least water and lowest hydration gradient than other sites. In all sites, the sky is dry outside and wet inside, which produces a positive gradient of

β . These results agree with the depth profiles obtained using Segmented Least-Squares fitting method[8].

5. Conclusion

We developed a new multi-layer mathematical model and an opto-thermal inverse depth profiling technique using a modified GA. Both the simulation results and the measurement results agree well with the given signal data, which shows that the new scheme developed is promising and effective to solve opto-thermal inverse problems.

Acknowledgments

The authors thank EPSRC, the Royal Society and South Bank University for financial support. We also thank CVCP for the ORS award to student Y. Cui.

References

1. R E Imhof, D J S Birch, F R Thornley, J R Gilchrist, and T A Strivens, J Phys E: Sci Instrum, 1984, **17**, 512-515.
2. P Xiao and R E Imhof, SPIE Proc., 1999, **3601**, 340-347.
3. R E Imhof, B Zhang, and DJS Birch, *Progress in Photothermal and Photoacoustic Science and Technology* (PTR Prentice Hall, Englewood Cliffs (USA), 1994), Vol. **II**, p.185-236.
4. Y Cui, P Xiao, R E Imhof, and C Glorieux, Review of Sci Instruments, 2003, **74**, 368-371.
5. A C Nearchou, Mech. Mach. Theory, 1998, **33**(3), 273-292.
6. A Homaifar, C R Houck and X Qi, Simulation, 1994, **62**(4), 242-254.
7. K Deb, Comput. Methods Appl. Mech. Engrg., 2000, **186**, 311-338.
8. P Xiao, J A Cowen, R E Imhof, Analytical Sci., 2001, **17**, 349-352.

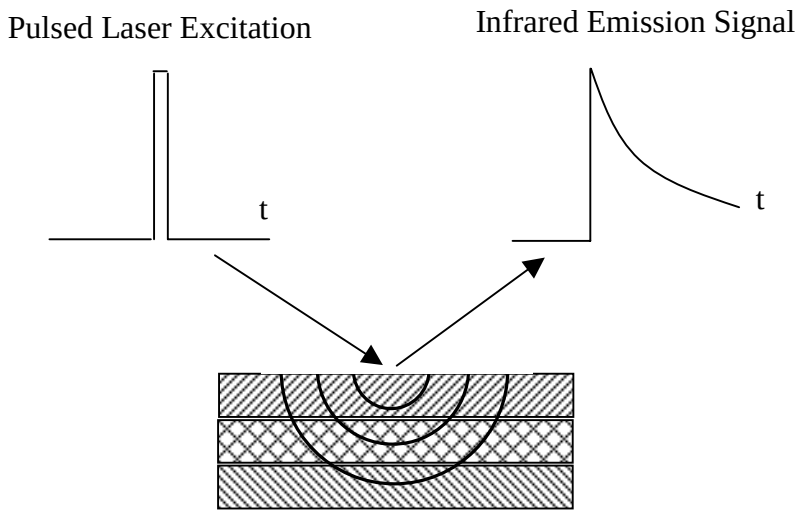

Fig. 1. Schematic diagram of OTTER measurement

```
procedure GA
begin
        gen=0
        Initialize Pop(gen)
        Evaluate Pop(gen)
        repeat
                gen=gen+1
                Select Pop(gen) from Pop(gen-1)
                Crossover Pop(gen)
                Mutate Pop(gen)
                Evaluate Pop(gen)
                Pop(gen-1)= Pop(gen)
        until (TerminationCondition)
end
```

Fig. 2. The basic structure of a genetic algorithm

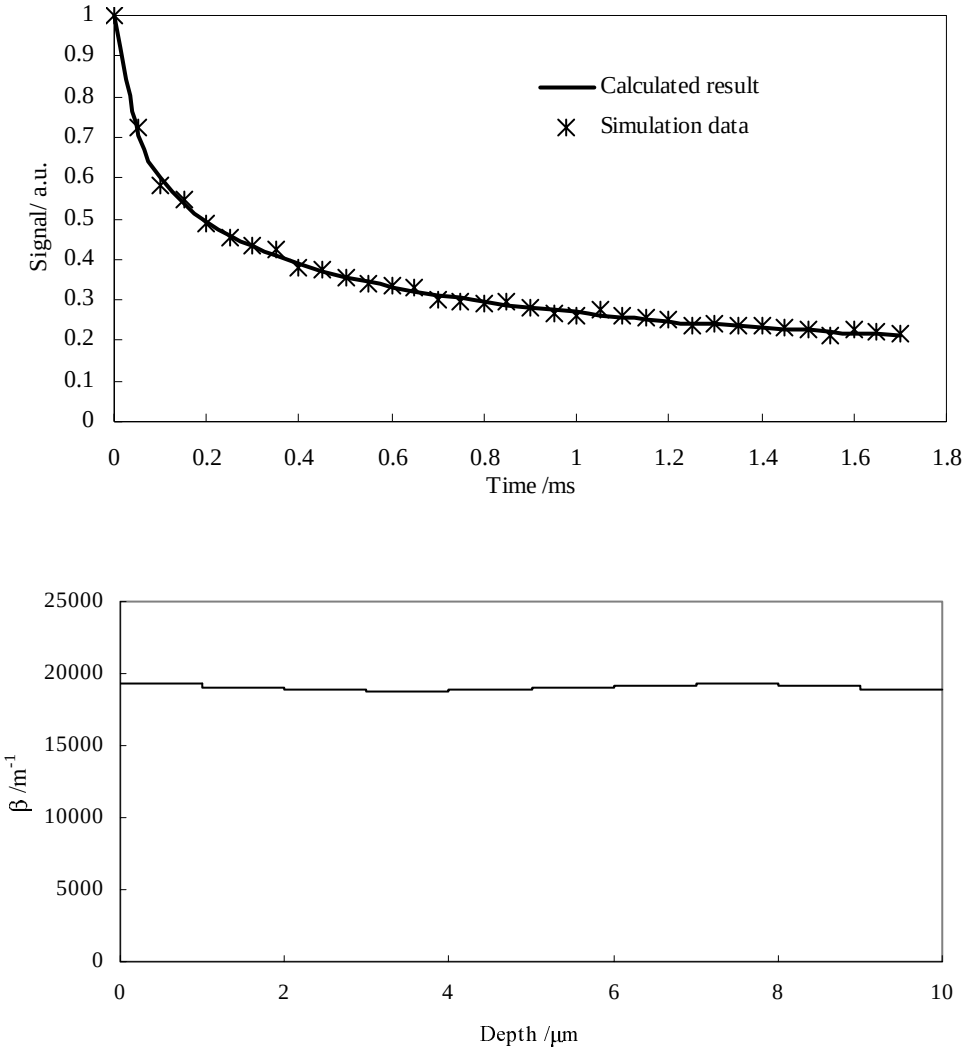

Fig. 3. Results for simulation data

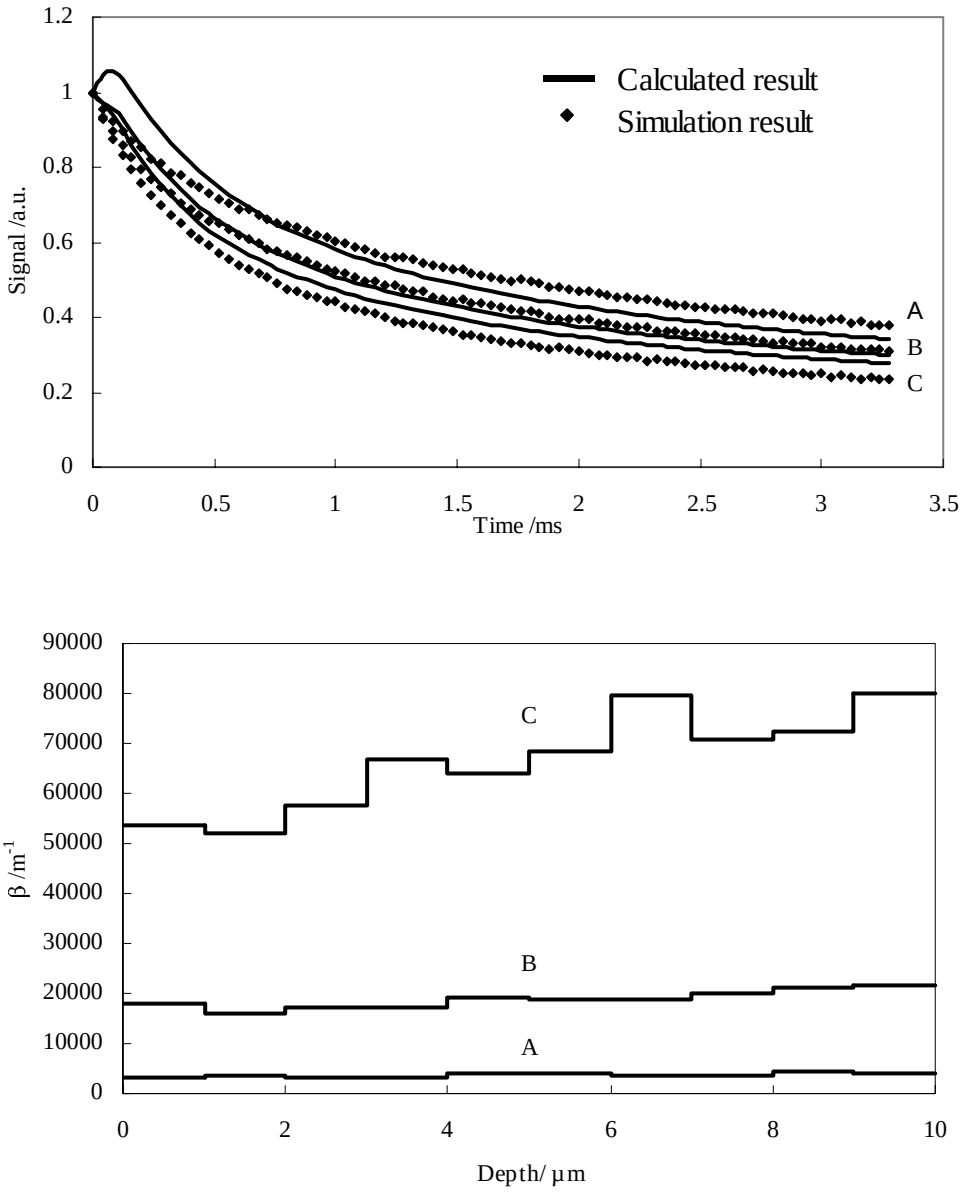

Fig. 4. Optical depth profiles of different skin sites.

(A) nail (B) palm (C) forearm